Self-Assembled Aggregates of the Carotenoid Zeaxanthin: Time-Resolved Study of Excited States

Helena Hörvin Billsten, Villy Sundström, and Tomáš Polívka*

Department of Chemical Physics, Lund University, P.O. Box 124, S-221 00 Lund, Sweden

Received: November 10, 2004; In Final Form: December 21, 2004

In this study, we present a way of controlling the formation of the two types of zeaxanthin aggregates in hydrated ethanol: J-zeaxanthin (head-to-tail aggregate, characteristic absorption band at 530 nm) and H-zeaxanthin (card-pack aggregate, characteristic absorption band at 400 nm). To control whether J- or H-zeaxanthin is formed, three parameters are important: (1) pH, that is, the ability to form a hydrogen bond; (2) the initial concentration of zeaxanthin, that is, the distance between zeaxanthin molecules; and (3) the ratio of ethanol/water. To create H-aggregates, the ability to form hydrogen bonds is crucial, while J-aggregates are preferentially formed when hydrogen-bond formation is prevented. Further, the formation of J-aggregates requires a high initial zeaxanthin concentration and a high ethanol/water ratio, while H-aggregates are formed under the opposite conditions. Time-resolved experiments revealed that excitation of the 530-nm band of J-zeaxanthin produces a different relaxation pattern than excitation at 485 and 400 nm, showing that the 530-nm band is not a vibrational band of the S_2 state but a separate excited state formed by J-type aggregation. The excited-state dynamics of zeaxanthin aggregates are affected by annihilation that occurs in both J- and H-aggregates. In H-aggregates, the dominant annihilation component is on the subpicosecond time scale, while the main annihilation component for the J-aggregate is 5 ps. The S_1 lifetimes of aggregates are longer than in solution, yielding 20 and 30 ps for H- and J-zeaxanthin, respectively. In addition, H-type aggregation promotes a new relaxation channel that forms the zeaxanthin triplet state.

1. Introduction

Carotenoids are a widespread and important group of pigments. They are present in most organisms, including humans, but can only be synthesized by plants and microorganisms.[1] In plants, they act as light harvesting pigments, covering efficiently the blue-green spectral region.[2] In addition to this function, they protect the plants against excessive light by regulating the flow of energy via singlet and triplet states of chlorophylls.[3] They are also known to be efficient quenchers of dangerous singlet oxygen and reactive radicals, by interrupting the chain of oxidative reactions.[4] In humans, the antioxidative function is probably the key mechanism in protection against various degenerative diseases such as cancer, atherosclerosis, and age-related macular degeneration.[5]

The diversity of carotenoid function is directly related to their unique excited-state properties that result from the carotenoid molecule having approximate C_{2h} symmetry. Thus, the electronic states of carotenoids are related to those of polyenes and the various functions of carotenoids depend mostly on the photophysical properties of the two lowest excited singlet states, denoted S_1 and S_2. A substantial amount of information has been gathered in the past decade about properties of excited states of carotenoids in both solution and proteins.[2] The strong absorption in the visible region arises from an allowed transition between the S_0 and the S_2 state. After being promoted into the S_2 state, the carotenoid molecule undergoes internal conversion on the 50−300 fs time scale to the lowest excited state, denoted S_1. A one-photon transition between the S_0 and the S_1 states is symmetry-forbidden, because the S_1 state has the same symmetry as the ground state. The lifetime of the S_1 state varies in the range from 1 to 300 ps, depending on the number of conjugated double bonds.[2]

While monomeric carotenoids have been the subject of numerous theoretical and experimental studies,[2] excited states of carotenoid aggregates are much less understood. It is well-known that carotenoids form aggregates when dissolved in hydrated polar solvents and that aggregation is characterized by dramatic changes in their absorption spectra.[6−8] Two types of carotenoid aggregates can be distinguished according to their absorption spectra. The first type is associated with a large blue shift of the absorption spectrum and loss of vibrational structure of the S_2 state. This type is suggested to be due to the so-called card-pack aggregates, in which the conjugated chains are oriented parallel to each other and are closely packed.[7] These aggregates are also called H-aggregates and the blue shift of the absorption spectrum is explained in terms of excitonic interaction between closely packed carotenoid molecules.[7] The second aggregation type is characterized by a red shift of the absorption spectrum, while the resolution of vibrational bands is preserved. This aggregation (J-type) is likely a result of a head-to-tail organization of conjugated chains, forming a loose association of carotenoid molecules.[7] The origin of the red shift is not well understood, but an increase of refractive index inside the aggregates was suggested as a possible explanation.[9] Moreover, carotenoid aggregates have been found to be chiral, although individual carotenoid molecules usually do not exhibit chirality. This phenomenon has been explained as due to a formation of large carotenoid assemblies having a helical structure.[7] The possibility of a long-range energy transfer within J-type carotenoid aggregates has been suggested,[9] but no time-

* Corresponding author: Fax +46-46-222-4119; e-mail tomas.polivka@chemphys.lu.se.

10.1021/jp044847j CCC: $30.25 © 2005 American Chemical Society
Published on Web 02/08/2005

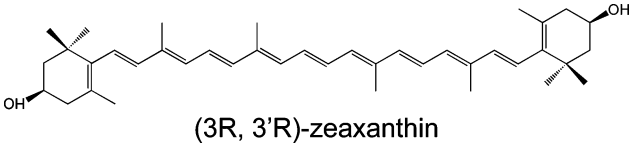

Figure 1. Molecular structure of (3*R*,3′*R*)-zeaxanthin.

resolved studies that would enable one to resolve such a process have been carried out so far.

Besides aggregation of carotenoids in hydrated solvents, it occurs also in various natural and artificial systems. Typically, carotenoids tend to aggregate when present in lipid bilayers, in which long-range organization of carotenoid molecules are believed to control physical and dynamical properties of lipid membranes[8] and protect them from lipid peroxidation.[10] In lipid bilayers, carotenoids usually form H-type aggregates.[8] However, it was recently shown that absorption changes consistent with J-type aggregation may occur as a result of carotenoid−protein interaction.[11,12] In artificial systems, H-aggregates are often formed when carotenoids are deposited on surfaces.[13,14] Since assemblies consisting of carotenoid molecules attached to conducting or semiconducting materials holds promise to act as photoactive species in dye-sensitized solar cells[15−17] or as molecular wires,[18] understanding the effects of aggregation on the structure of excited states is an important factor in controlling the efficiency of such devices.

Aggregates of the carotenoid zeaxanthin (molecular structure in Figure 1), which is the subject of this study, are interesting for several reasons. First, zeaxanthin forms aggregates more readily than other carotenoids.[6] Moreover, zeaxanthin can form both J- and H-aggregates (denoted hereafter as J-zeaxanthin and H-zeaxanthin).[6,11,12] Yet it is not well understood what parameters control whether J- or H-zeaxanthin is formed. Second, zeaxanthin aggregates are suggested to play important physiological roles. In plants, zeaxanthin is a part of the xanthophyll cycle that is a key component of plant photoprotection.[3] The xanthophyll cycle involves light-dependent enzymatic interconversion of three xanthophylls (zeaxanthin, antheraxanthin, and violaxanthin) that requires decoupling of the carotenoids from proteins and their release into lipid membranes, in which aggregation may occur.[8] Zeaxanthin, produced under high-light conditions in the xanthophyll cycle, is required for direct dissipation of energy via quenching of chlorophyll excited states, the so-called nonphotochemical quenching (NPQ).[3] Although details about the NPQ mechanism are still elusive, it is clear that quenching conditions correlate with an absorption change at 535 nm.[19] Recently, this absorption change was hypothesized to be a result of binding of zeaxanthin to the PsbS protein, which is another required component of the NPQ.[20] The formation of the zeaxanthin−PsbS complex induces changes in the absorption spectrum of zeaxanthin that are nearly identical to those of J-zeaxanthin, possessing a characteristic band at around 530 nm.[11] Since increased levels of the PsbS protein have also been suggested to induce a direct quenching of chlorophyll excited states via energy and/or electron transfer to zeaxanthin,[21] studies of the zeaxanthin excited states under aggregation conditions may provide important information about quenching mechanisms.

Zeaxanthin aggregates are also interesting in relation to their possible roles in the vision apparatus of humans. Zeaxanthin is selectively accumulated in the foveal region of the macula of the human eye, likely acting as a photoprotective pigment.[22] It was shown that zeaxanthin is bound to a specific membrane-associated xanthophyll-binding protein (XBP). Interestingly, binding of zeaxanthin to XBP results in a monomeric zeaxanthin absorption spectrum,[22,23] while binding of zeaxanthin to another macular protein, glutathione S-transferase (GSTP1), leads to a J-zeaxanthin spectrum essentially identical to that of the zeaxanthin−PsbS complex of higher plants.[12] In addition, zeaxanthin in the eye occurs also in lipid membranes, in which formation of H-zeaxanthin dominates.[24] It was also shown that singlet oxygen quenching exhibits an anomalous dependence on the zeaxanthin concentration in liposomes. Decrease of singlet oxygen quenching efficiency at higher zeaxanthin concentrations was explained as due to a greater aggregation tendency of zeaxanthin than for other carotenoids. The aggregation state of zeaxanthin may thus control the efficiency of singlet oxygen scavenging.[25]

In this work, we focus on investigation of zeaxanthin aggregates by a combination of steady-state and transient absorption techniques, aiming for a better understanding of their excited-state properties. First, we present a well-defined way of controlling formation of either H- or J-zeaxanthin in hydrated ethanol. Then, having established the conditions for producing both types of aggregates, we apply time-resolved absorption spectroscopy to monitor properties of the lowest excited state of H- and J-zeaxanthin. The results are compared with those obtained for monomeric zeaxanthin in solution and related to possible functions of zeaxanthin aggregates in various systems.

2. Experimental Section

Zeaxanthin (Hoffman-LaRoche) was dissolved in ethanol to achieve samples with concentrations of 50, 65, or 100 μM. Mixtures of water and ethanol were made by addition of deionized water to a final content of 20%, 40%, 60%, or 80% to stock solutions of ethanol, containing 50 or 100 μM zeaxanthin. Experiments on pH dependence were made by addition of water with pH 4.0, 7.0, 8.5, or 10.0 ($\pm$0.2) to samples of zeaxanthin (65 μM) in 100% ethanol (the desired pH was achieved through addition of concentrated NaOH and HCl), and the pH of the water was measured by use of a Metrohm pH-meter.

The femtosecond spectrometer used in these studies is based on an amplified Ti:sapphire laser system, producing $\sim$120 fs pulses at 5 kHz repetition rate with an average output power of 0.2 mJ/pulse and a central wavelength of 800 nm. For measurements of transient absorption spectra, the amplified pulses were divided into two paths, one to pump an optical parametric amplifier to generate excitation pulses at 490 nm and the other one to produce white-light continuum probe pulses in a 0.5 cm sapphire plate. The relative polarization of the excitation and probe beams was set to the magic angle (54.7°). Absorption spectra were measured before and after measurements to ensure that no photochemical damage occurred during the experiments. While both zeaxanthin and H-zeaxanthin were very stable throughout the measurements, J-zeaxanthin was sensitive to laser light and fresh samples had to be prepared regularly. All measurements were performed in a 2 mm path length glass cuvette at 293 K.

3. Results

Steady-State Absorption. To investigate conditions that determine formation of either H-zeaxanthin or J-zeaxanthin, absorption spectra of zeaxanthin were measured for various water/ethanol mixtures and various initial concentrations of zeaxanthin. The results of two different initial concentrations of zeaxanthin are shown in Figure 2. For the 50 μM ethanol solution of zeaxanthin (Figure 2a), addition of water up to 20% has essentially no effect on the absorption spectrum. When the

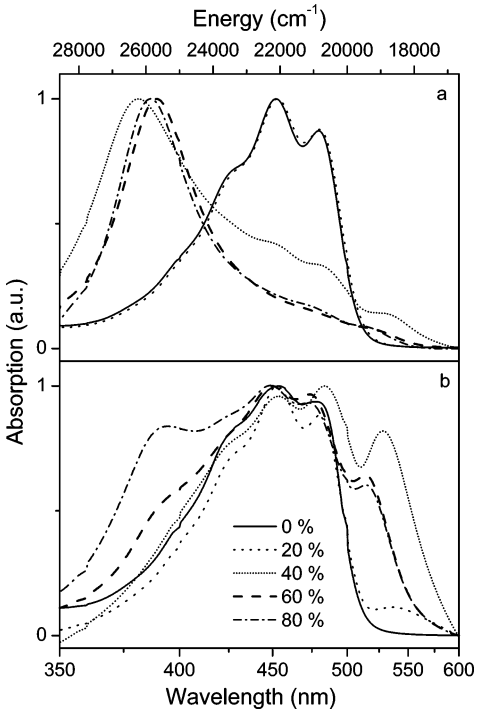

Figure 2. Steady-state absorption spectra of zeaxanthin at different water concentrations. Initial concentration of zeaxanthin in ethanol was 50 μM (a) and 100 μM (b). All absorption spectra are normalized.

water content is increased to 40%, the characteristic absorbance between 400 and 500 nm is suppressed, though vibrational bands of the S_2 state are still visible, and the formation of a new feature typical for H-zeaxanthin appears. Further increase of the water content stabilizes H-zeaxanthin as the vibrational structure disappears and a distinct absorption band at 390 nm dominates the absorption spectrum. It is worth noting that a weak new band is also formed at 525 nm and this band is most pronounced at a water concentration of 40%. When the initial concentration of zeaxanthin is increased to 100 μM (Figure 2b), a distinctly different dependence on water content is observed. This high concentration leads to a slight decrease of resolution of vibrational bands even in ethanol. However, at a water content of 20%, the resolution of the structure is restored and a new broad band at 540 nm corresponding to J-zeaxanthin appears. Increasing the water content from 20% to 40% clearly stabilizes J-zeaxanthin since the relative amplitude of the red band increases several times. Simultaneously, this band is shifted to 530 nm. There is also a visual change in coloration, from dark yellow to red/orange, and the solution turns slightly opaque. When the water content is increased, the magnitude of the red band is decreased and a distinct feature at 390 nm grows, signaling the formation of H-zeaxanthin. At a water content of 80% the sample contains a mixture of both J- and H-zeaxanthin. In agreement with previous observations,[7] formation of J-zeaxanthin preserves resolution of vibrational bands.

When exploring various conditions for zeaxanthin aggregate formation, we found that the pH of the water added to the ethanol solution of zeaxanthin plays an important role in determining whether H- or J-zeaxanthin is formed. A high initial zeaxanthin concentration is a key factor to produce J-zeaxanthin, but it is not sufficient unless the added water has a proper pH. This is shown in Figure 3, where absorption spectra of zeaxanthin in hydrated ethanol are shown for different pH values. To demonstrate the importance of pH, an initial zeaxanthin concentration of 65 μM was used, because at this concentration it is possible to form both J- and H-zeaxanthin.

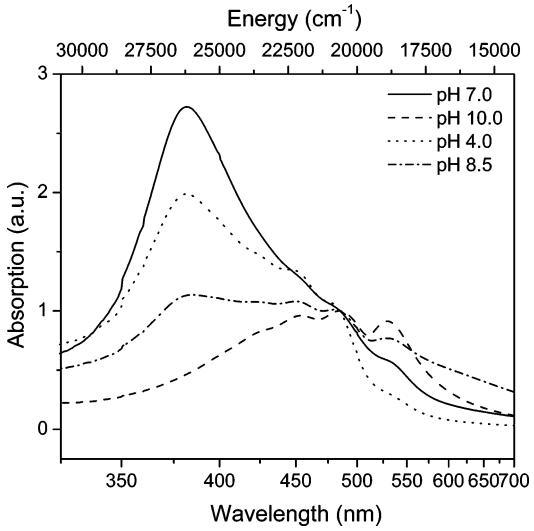

Figure 3. Steady-state absorption spectra of zeaxanthin in 40% water at various pH values. Initial concentration of zeaxanthin was 65 μM.

To induce aggregation, water of various pH was added to a final concentration of 40%. In this mixture, one could expect the red aggregates to be the dominant feature (see above). However, addition of water at neutral pH clearly produces H-zeaxanthin as the band at 390 nm dominates the absorption spectrum. A fraction of J-zeaxanthin could also be present since a weak band at ~530 nm is also visible. When the water is more acidic (pH ~ 4), the red band disappears completely and the 390-nm band decreases along with appearance of a hint of monomeric vibrational structure, indicating that acidic water prevents both types of aggregation. On the other hand, addition of water with pH ~ 8.5 favors formation of J-zeaxanthin. Further increase of pH to ~10 produces solely J-zeaxanthin, as the 390-nm absorption band disappears completely and vibrational structure is restored.

On the basis of these results, we used the following conditions for preparation of samples for time-resolved measurements. H-Zeaxanthin was prepared from an initial concentration of 50 μM by adding water of neutral pH to a final water content of 80%. J-Zeaxanthin was prepared from an initial concentration of 100 μM by adding water of pH ~ 8.5 to a final water content of 40%. This preparation procedure produced aggregates whose absorption spectra are in Figure 4 compared with the absorption spectrum of a 50 μM solution of zeaxanthin in ethanol (hereafter referred to as zeaxanthin). Zeaxanthin shows strong absorption in the 350−550-nm region associated with the allowed S_0-S_2 transition. The spectrum exhibits the characteristic three-peak structure of carotenoids due to vibrational structure of the S_2 state. The vibrational peaks are located at 480 (0-0), 450 (0-1), and 425 nm (0-2). For J-zeaxanthin, the vibrational structure is preserved but the absorption spectrum is markedly broader. The characteristic band of J-zeaxanthin is located at 530 nm and it is accompanied by a long absorption tail extending beyond 700 nm. It is worth noting that, except for the 530-nm band, the vibrational bands are located at nearly the same positions as for zeaxanthin. H-Zeaxanthin exhibits an absorption spectrum dominated by a structureless sharp band located at 390 nm. This band also possesses a red wing extending beyond 500 nm, with a hint of weak shoulders located at 480 and 530 nm. It is worth mentioning that higher excited states are affected in different ways depending on the type of aggregation. The spectral band peaking for zeaxanthin at 278 nm (the first allowed excited state above the S_2 state), is negligibly influenced by the formation of H-zeaxanthin, while J-zeaxanthin induces changes similar

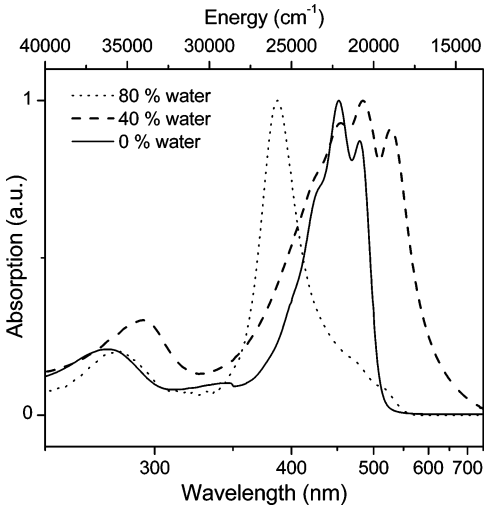

Figure 4. Steady-state absorption spectra of monomeric zeaxanthin (solid line, concentration 50 μM, water concentration 0%), J-zeaxanthin (dashed, 100 μM, 40%), and H-zeaxanthin (dotted, 50 μM, 80%) at 293 K.

to those observed for the S_2 state; the absorption band is broadened and its maximum is red-shifted, peaking at 298 nm.

Transient Absorption. To obtain knowledge about the excited states of the zeaxanthin aggregates, transient absorption spectra were recorded in the spectral region 470−700 nm (Figure 5a). For all three forms of zeaxanthin, the transient spectra were measured at 3 ps after excitation at 400 nm (H-zeaxanthin), 485 nm (zeaxanthin), and 525 nm (J-zeaxanthin). In agreement with previously published results,[26,27] the transient absorption spectrum of zeaxanthin is dominated by an excited-state absorption (ESA) band peaking at 555 nm, which reflects the spectral profile of the S_1-S_N transition. For H-zeaxanthin, the peak position of the main ESA band (560 nm) is close to that of zeaxanthin, but the spectral band is markedly broader at the lower energy side. In fact, the ESA band of H-zeaxanthin is broadened also toward higher energies, but a negative band centered at 525 nm is superimposed on the high-energy ving of the ESA spectrum, giving the impression of a separate ESA band at ∼500 nm. This negative feature originates from a ground-state bleach of the weak 525-nm band of H-zeaxanthin (Figure 4). For J-zeaxanthin, the ESA band is further red-shifted, peaking at 605 nm, and similarly to H-zeaxanthin it has a red tail extending beyond 700 nm. The strong negative feature at ∼540 nm is due to ground-state bleaching of the characteristic red absorption band of J-zeaxanthin (see Figure 4 for absorption spectrum).

Kinetics recorded at the maxima of the ESA bands of the different zeaxanthin species, monitoring dynamics of the lowest excited state, reveals further differences (Figure 5b). The zeaxanthin S_1 state decays monoexponentially with a time constant of ∼9 ps, in agreement with results obtained for zeaxanthin in various solvents.[28] For J-zeaxanthin, however, two decay components of 4.7 and 30 ps are needed to fit the kinetics. The S_1 decay of H-zeaxanthin is even more complicated and at least four decay components are required to obtain a satisfactory fit. A time constant of 0.5 ps represents the major component of the decay, accompanied by two slower components of 4.5 and 20 ps. To account for the rest of the decay, a longer component (∼500 ps) must be added. Identical kinetics were obtained when probing at 505 nm (see Table 1), confirming that the 505-nm feature is not a distinct spectral band but is indeed created as a result of overlapping ESA and bleaching bands. It is also important to note that while the zeaxanthin

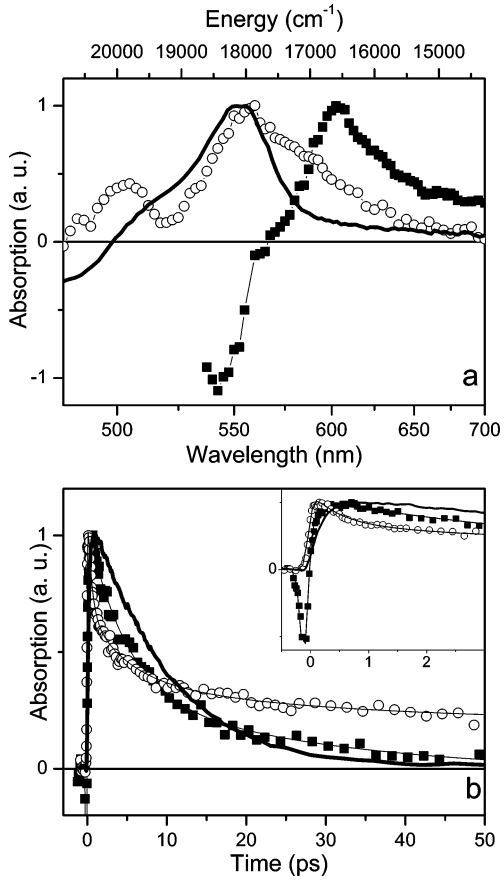

Figure 5. (a) Transient absorption spectra of monomeric zeaxanthin (—, excitation at 485 nm), H-zeaxanthin (○, excitation at 400 nm) and J-zeaxanthin (■, excitation at 525 nm). All transient spectra were recorded 3 ps after excitation and normalized to maximum. (b) Kinetics recorded for all three samples at the corresponding maxima of their transient absorption spectra: zeaxanthin (—, probe at 555 nm), H-zeaxanthin (○, 560 nm), and J-zeaxanthin (■, 605 nm). Solid lines through symbols correspond to fits. Early time dynamics is shown in the inset.

and the J-zeaxanthin kinetics contain a ∼250 fs rise component that is usually assigned to the S_2-S_1 decay, this rise component is substantially shorter for H-zeaxanthin, challenging our time resolution of ∼100 fs. The fitting results are summarized in Table 1.

To obtain further insight into the excited-state properties, transient absorption spectra of J-zeaxanthin were also measured after excitation at 400 and 485 nm and compared to the spectrum obtained after excitation into the red band (525 nm). The results are shown in Figure 6. It is apparent that moving the excitation to higher energies changes the S_1-S_N spectral profile significantly. Both 400- and 485-nm excitation produce a transient absorption spectrum containing two spectral bands. A new band centered at 560 nm appears in the transient spectra recorded after 400- and 485-nm excitation. In fact, this band could be interpreted as due to the S_1-S_N transition of zeaxanthin (see Figure 5a), with the 605-nm band of J-zeaxanthin superimposed as a shoulder.

Therefore, to establish the origin of the 560-nm band in the transient absorption spectrum of J-zeaxanthin, kinetics were measured at 560 and 605 nm after 400-nm excitation (Figure 7). While the 605-nm band exhibits a decay that is almost identical to that recorded after excitation at 525 nm (see Figure 5b and Table 1), probing at 560 nm results in different kinetics; a multiexponential fit gives a time constant of 9 ps for the shorter component, while the longer has a time constant of 30 ps. Thus,

TABLE 1: Results of the Multiexponential Fitting[a]

sample	λ_{exc} (nm)	λ_{pr} (nm)	τ_0 (ps)	τ_1 (ps)	τ_2 (ps)	τ_3 (ps)	τ_4 (ps)
Zea	485	560	0.29 (−100)		9.3 (100)		
J-Zea	400	560	0.12 (−40)	0.7 (−40)	9 (64)	30 (36)	
J-Zea	400	605	0.13 (−100)	0.35 (15)	4.8 (62)	30 (23)	
J-Zea	485	560	0.1 (−60)	0.7 (−30)	9 (93)	30 (7)	
J-Zea	485	605	0.11 (−100)		4.5 (57)	30 (43)	
J-Zea	525	605	0.22 (−20)		4.8 (67)	30 (33)	
H-Zea	400	505	<0.09 (−100)	0.3 (50)	4.4 (23)	20 (7)	>500 (20)
H-Zea	400	560	<0.09 (−100)	0.5 (41)	4.5 (23)	20 (15)	>500 (21)
H-Zea	400	600	<0.09 (−100)	0.4 (66)	4.5 (11)	23 (23)	

[a] Numbers in parentheses correspond to relative amplitudes (%) of the fitting components; uncertainties of the time constants and amplitudes vary between 10% and 15%.

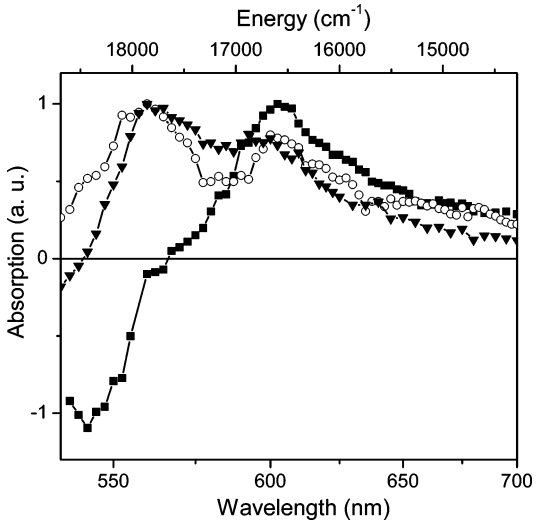

Figure 6. Transient absorption spectra of J-zeaxanthin recorded at 3 ps after excitation at 525 nm (■), 485 nm (○), and 400 nm (▼). All spectra are normalized to maximum.

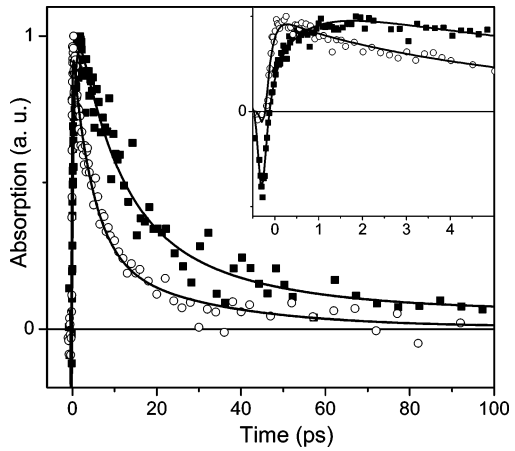

Figure 7. Kinetics of J-zeaxanthin measured at 560 nm (■) and 605 nm (○) after excitation at 400 nm. Solid lines represent multiexponential fits of the data. The inset shows enlargement of the first few picoseconds. Kinetics is normalized.

while the longer component in the 560-nm decay resembles that of the 605-nm kinetics, the shorter component is very close to the S_1 lifetime of zeaxanthin. In addition, the 560-nm kinetics contains a pronounced 0.7-ps rise component that is missing in the kinetics recorded at 605 nm. A similar picture is obtained from fitting of kinetics measured at 605 and 560 nm after excitation of J-zeaxanthin at 485 nm (Table 1).

The different decays of the 560- and 605-nm bands of J-zeaxanthin prove their different origin and show that the 560-nm band is due to nonaggregated zeaxanthin. The presence of a fraction of H-zeaxanthin in the J-zeaxanthin sample can be safely ruled out, because a comparison of kinetics measured at 560 nm after 400-nm excitation of H- and J-zeaxanthin in Figure 8 shows that the decay of the 560-nm band of J-zeaxanthin cannot be interpreted as due to contamination of the sample by H-zeaxanthin. The decays of the S_1-S_N ESA of these two samples are strikingly different as both the fast (0.5 ps) decay and the very long (∼500 ps) components characteristic of H-zeaxanthin (Figure 5b and Table 1) are missing in the 560-nm kinetics of J-zeaxanthin. In addition, the 560-nm kinetics of J-zeaxanthin also contains a distinct subpicosecond rise that is absent in the kinetics of H-zeaxanthin.

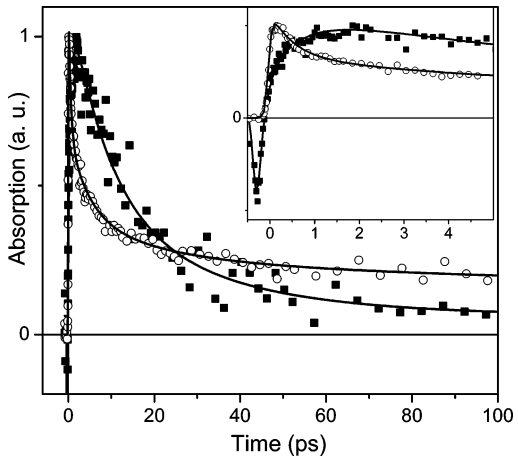

Figure 8. Kinetics along with fits (—) of H-zeaxanthin (○) and J-zeaxanthin (■) measured at 560 nm after excitation at 400 nm. The inset shows the dynamics during the first 5 ps.

Discussion

Formation of Aggregates. The carotenoid zeaxanthin has earlier been shown to form H-aggregates very easily in hydrated solvents,[6] but the absorption spectrum corresponding to J-zeaxanthin has been so far observed only when zeaxanthin molecules interact with some proteins.[11,12] Here we show that both types of zeaxanthin aggregates can be produced in hydrated ethanol, but formation of J-zeaxanthin requires specific conditions. The crucial factor is a proper pH that is directly related to the ability of zeaxanthin to form a hydrogen bond, because increasing pH causes deprotonation of the hydroxyl groups of zeaxanthin. At higher pH zeaxanthin is not able to create hydrogen bonds, which clearly favors formation of J-zeaxanthin, indicating that the head-to-tail aggregates can be formed only in the absence of hydrogen bonding. On the other hand, the pH dependence supports the earlier hypothesis that the card-pack H-aggregates are held together via a hydrogen-bonding network.[7,29,30] It is worth mentioning that similar results were obtained by Simonyi et al.,[7] who showed that for the carotenoids

lutein and capsanthol the presence of free hydroxyl groups produces solely H-aggregates, while acetylation of the hydroxyl groups favors formation of J-aggregates. These results are essentially the same as ours, except Simonyi et al. achieved the inhibition of hydrogen bonding by modification of the molecules, while here we showed that a pH change can control the aggregation type of the same carotenoid. In conclusion, the ability of hydrogen-bond formation is a decisive factor for whether J- or H-aggregates are formed. The necessity of hydrogen bonding for H-zeaxanthin formation can be justified by the expected card-pack structure of the aggregates. As shown by Simonyi et al.[7] for other carotenoids, the presence of a free hydroxyl group at both sides of a carotenoid molecule is necessary for the formation of H-aggregates. Therefore, in the simple case of a dimer, hydrogen bonding at both sides of the zeaxanthin molecule helps to keep the two molecules together lying on top of each other with their dipoles oriented almost perfectly parallel to each other. It is, however, worth noting that other molecular forces such as $\pi-\pi$ stacking interactions may contribute significantly to the attractive forces between closely packed carotenoid molecules.[31] These attractive forces are stronger when molecules are planar, explaining why zeaxanthin, having a rigid planar structure, forms H-aggregates more readily than other carotenoids.[6] On the contrary, weak van der Waals interactions dominate in J-zeaxanthin, which results in lower stability of these aggregates.

The different structures of H- and J-aggregates also explain the different ethanol/water ratios that are optimal for the formation of either H- or J-zeaxanthin. The strong hydrophobia of carotenoids forces the conjugated backbone of carotenoids to avoid contact with water molecules. Because of the head-to-tail structure of J-zeaxanthin, the conjugated chains are inevitably exposed to solvent. Therefore, rather low water content (optimal ethanol/water ratio of $\sim$1.5) is necessary to form J-zeaxanthin (see Figure 2b). Increasing the water content destabilizes J-zeaxanthin, as an increasing number of water molecules in the proximity of zeaxanthin compel the head-to-tail assembly to transform into the card-pack arrangement that pushes the water molecules away from the conjugated chains. The critical water content that initiates transformation of J-zeaxanthin to H-zeaxanthin depends on pH. For pH = $\sim$8.5 used in Figure 2b, the critical ethanol/water ratio is $\sim$0.65. For even higher pH values, the critical value is lower, but J-zeaxanthin becomes less stable. Nonetheless, to stabilize H-zeaxanthin, the optimal ethanol/water ratio lies in the range 0.2−0.3, in agreement with previous results.[6]

Another important factor controlling the formation of aggregates is the initial concentration of zeaxanthin in solution. Apparently, to stimulate J-zeaxanthin formation, the molecules must be close to each other already in ethanol solution. Again, this observation is consistent with the structures of zeaxanthin aggregates. At initial concentrations as high as 100 μM, the proximity of the zeaxanthin molecules in solution can be inferred from a slight loss of vibrational structure of the S_2 state (Figure 2b). This is most likely caused by a broader distribution of conformers resulting from steric hindrance between the molecules nearby. In such a situation, adding a moderate amount of water will push the zeaxanthin molecules close enough to form the head-to-tail aggregates without the conjugated chains being exposed to water. This leads to an arrangement of large assemblies as evidenced by the solution turning slightly opaque upon J-zeaxanthin formation. On the other hand, when the initial concentration drops below a certain level, a moderate water content is not enough to push the molecules close enough to form aggregates, and increasing the water content further will only lead to H-zeaxanthin formation, since the card-pack assemblies ensure the best protection against contact with water molecules. Thus, to summarize this section, there are three key factors controlling whether J- or H-zeaxanthin is formed: pH, ethanol/water ratio, and initial concentration of zeaxanthin in solution. The critical values of these factors are dependent on each other, but it is apparent that neutral pH, low zeaxanthin concentration, and low ethanol/water ratio promotes formation of H-zeaxanthin, while high values of these parameters give rise to J-zeaxanthin.

Origin of Spectral Changes. Since absorption changes of zeaxanthin consistent with formation of J-zeaxanthin have been recently proposed to play important physiological roles,[11,12] we first discuss the J-zeaxanthin properties. Although J-zeaxanthin has not been observed in hydrated solvents so far, we will make use of earlier results on J-aggregates of other carotenoids.[7,9] A common interpretation of absorption changes induced by formation of J-aggregates of carotenoids is that the absorption spectrum results from a red shift of the vibrational bands. If we apply this interpretation to J-zeaxanthin, then the redmost band at 530 nm is assigned to the 0-0 vibrational band. The same argument was also used to explain the 525-nm band induced by zeaxanthin−protein interaction.[11] However, comparison of the absorption spectra of zeaxanthin and J-zeaxanthin in Figure 4 does not fully support this explanation. First, while a large red shift is required to explain the low-energy part, the high-energy part seems to be rather blue-shifted upon formation of J-aggregates. Second, if the 530-nm band were due to the 0-0 vibrational band, then the energy gap between the 0-0 and 0-1 vibrational bands would be $\sim$1700 cm^{-1}, thus larger than the $\sim$1400 cm^{-1} between the 0-1 and 0-2 vibrational bands (Figure 4). A comparable mismatch between energy gaps exists also for J-aggregates of other carotenoids,[7,9] and the same problem arises when the absorption spectrum of a zeaxanthin−protein complex is explained this way.[11] Moreover, it is clear from Figure 2b that both spectral position and relative intensity of the lowest energy band of J-zeaxanthin depends on preparation method. Thus, the properties of this band are not consistent with the behavior expected for a vibrational band.

This hypothesis is further supported by the time-resolved data since excitation at 525 nm results in a markedly different transient absorption spectrum than that obtained after excitation at 485 or 400 nm (Figure 6). Excitation of the 530-nm band results in an ESA spectrum peaking at 605 nm that clearly is due to J-zeaxanthin as it shows no resemblance to the S_1-S_N ESA spectrum of monomeric carotenoids, neither in position nor in shape. In addition, the distinct bleaching band below 550 nm confirms that this spectrum indeed originates from molecules forming the characteristic red band of J-aggregates. On the contrary, the ESA spectra generated after 400- and 485-nm excitation are dominated by a band at 560 nm, which is very close to that of monomeric zeaxanthin (Figure 5a). Although H-zeaxanthin has an ESA band at the same position (Figure 5a), kinetics measured at 560 nm excludes this band as due to H-zeaxanthin; the 9 ps decay component that is present only at 560 nm after 400- and 485-nm excitation (see Table 1) matches well the known S_1 lifetime of monomeric zeaxanthin in solution. However, the kinetics also contains a 0.7 ps rise whose origin remains unknown. It is too long to be due to S_2-S_1 internal conversion,[2] and although it closely matches the vibrational relaxation in the zeaxanthin S_1 state,[28] this process should not be exhibited as a rise. A possible explanation could be related to release of a zeaxanthin molecule from J-zeaxanthin induced

by excitation, giving rise to the ESA band of monomeric zeaxanthin, but further experimental work is needed to test the feasibility of such a hypothesis.

Thus, on the basis of the excitation wavelength dependence, one can conclude that while excitation at 525 nm excites selectively J-zeaxanthin, moving the excitation to higher energies results in excited-state dynamics corresponding to zeaxanthin in solution. This further strengthens our proposal that monomeric zeaxanthin contributes to the absorption spectrum of J-zeaxanthin shown in Figure 4. Nevertheless, the presence of a shoulder at 605 nm in the transient absorption spectrum after 400- and 485-nm excitation shows that J-zeaxanthin has an absorption extending to 400 nm. From the amplitudes of the 9 ps component in the decays after 400- and 485-nm excitation (Table 1), it may be concluded that the absorption of J-zeaxanthin decreases toward shorter wavelengths, which is also justified by the absence of a bleaching band below 550 nm after 400- and 485-nm excitation.

Our results suggest that what is generally considered as the absorption spectrum of a J-aggregate of a carotenoid actually consists of contributions from the J-aggregate and the monomeric carotenoid. Thus, the absorption spectrum of J-zeaxanthin is dominated by a distinct band at 530 nm, which possesses a tail extending to higher energies. Such a situation suggests interpretation of the absorption spectrum of zeaxanthin aggregates in terms of excitonic interaction between zeaxanthin molecules. In the excitonic picture, H-zeaxanthin results in excitonic splitting with the upper exciton band allowed, while interaction between molecules within J-zeaxanthin leads to the allowed lower exciton band. This explanation has been generally accepted for H-aggregates of carotenoids, because modeling of the absorption spectrum of H-aggregates of lutein by an excitonically coupled dimer was successfully achieved by Zsila et al.[9] Assuming a tightly packed dimer in which lutein molecules are ~5.5 Å apart and oriented parallel to each other, these authors showed that the resulting excitonic splitting reproduces well the measured absorption spectrum. Accordingly, we assign the strong band of H-zeaxanthin at 390 nm to the upper exciton component of strongly coupled zeaxanthin molecules, forming card-pack aggregates.[32,33] Although the spectrum can be in the first approximation reproduced by a dimer, it is expected that H-aggregates of carotenoids consist of a broader distribution of sizes as evidenced by atomic force microscopic images.[9] For J-aggregates of carotenoids, however, the previous interpretations of the absorption spectrum as due to a red shift of the whole absorption band did not favor excitonic splitting as an explanation of the observed absorption changes. Instead, an enhancement of the refractive index inside the J-aggregates was proposed to be a possible origin.[9] However, as our results suggest that the formation of J-zeaxanthin is not due to a red shift of the zeaxanthin absorption spectrum but rather due to appearance of a new band located around 530 nm, the excitonic splitting with the lower component allowed seems to be the most likely explanation. The same interpretation was suggested to explain the CD spectrum of the zeaxanthin−PsbS complex, for which a weakly interacting zeaxanthin dimer, with the lower excitonic component located at 535 nm, was used to reproduce the CD spectrum.[11]

Excited-State Dynamics. Excited state processes in aggregates usually contain a significant contribution from exciton−exciton annihilation.[34,35] The multiexponential decays observed for both H- and J-zeaxanthin are consistent with the annihilation dynamics. In both cases, the major decay component is faster than the S_1 lifetime of monomeric zeaxanthin, suggesting a loss

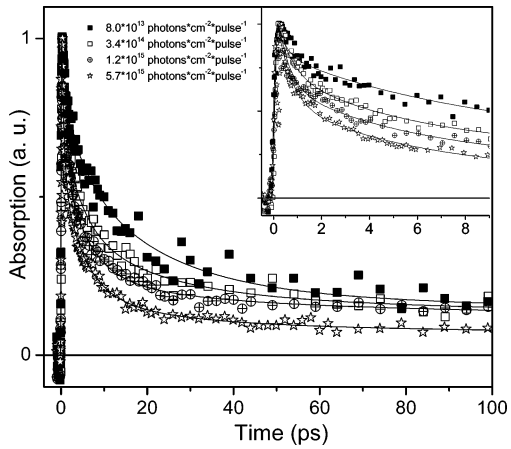

Figure 9. Kinetics along with fits (−) of H-zeaxanthin measured at 560 nm after excitation at 400 nm with different excitation pulse intensities. The inset shows the dynamics of the first 10 ps.

TABLE 2: Global Fitting of Excitation Intensity Dependence for H-Zeaxanthin[a]

I_{exc} (nJ/pulse)	$\tau_1 = 0.5$ ps	$\tau_2 = 5$ ps	$\tau_3 = 20$ ps	$\tau_1 > 500$ ps
30	26	17	39	18
120	32	30	22	17
400	36	42	12	11
2000	44	30	10	17

[a] Kinetics was recorded at 560 nm after 400-nm excitation. Numbers correspond to relative amplitudes (%) of the fitting components.

of excited-state population via annihilation. To confirm this conjecture, we have measured decay of the S_1-S_N ESA band of H-zeaxanthin upon varying the intensity of the 400-nm excitation. The obtained kinetics are shown in Figure 9 and the results of a global fitting analysis are summarized in Table 2. The results confirm that at least the two fastest components are due to annihilation, because their amplitudes increase with the increase of excitation intensity. Since it is expected that a distribution of aggregates with various sizes exists in the sample, the 0.5 ps component is likely related to annihilation within smaller aggregates consisting of a few molecules within the card-pack aggregate. In such an aggregate, excitation migrates only a short distance prior to the annihilation. On the other hand, the 5 ps component may be assigned to a long-range annihilation occurring in larger aggregates, in which excitations created in the H-zeaxanthin must travel across a number of zeaxanthin molecules to reach the annihilation site.

The third 20 ps component exhibits opposite dependence of its amplitude on excitation intensity. Such dependence is expected for the intrinsic S_1 lifetime of a zeaxanthin within the H-aggregate. At lower intensities, there is lower probability of annihilation, thus a large fraction of zeaxanthin decays to the ground state with its true S_1 lifetime. Increasing excitation intensity also increases the probability of annihilation; thus the proportion of molecules decaying to the ground state prior to annihilation decreases correspondingly. Thus, we assign the 20 ps component, which is about two times longer than the S_1 lifetime of monomeric zeaxanthin, to the S_1 lifetime of zeaxanthin in H-aggregate (Table 1). This difference can be explained by restrained vibrational motion of individual zeaxanthin molecules within H-zeaxanthin. It is a well-established fact that the S_1 decay is driven by vibrational coupling to the ground state via the C=C stretching mode.[36] Consequently, disturbing the vibrational motion of the conjugated backbone, for example, by substituting carbons in the conjugated chain by the heavier ^{13}C, leads to a slower S_1 lifetime.[36] Similar effect

may occur when zeaxanthin molecules are tightly packed within H-zeaxanthin, moreover bound together by hydrogen bonds (see above). Such arrangement hinders vibrational motion of the conjugated backbone, explaining why the S_1 lifetime is longer than for monomeric zeaxanthin.

For J-zeaxanthin, the excitation intensity dependence could not be performed, because J-zeaxanthin was not stable under higher excitation intensities. Nevertheless, it is likely that the 5 ps component is related to annihilation. The missing subpicosecond component is likely a result of the weaker interaction between zeaxanthin molecules in the head-to-tail arrangement of J-zeaxanthin, although it may be also explained by the fact that the J-zeaxanthin sample is dominated by large assemblies and there is little chance that at modest excitation intensity two excitations will be close enough for fast annihilation. Similarly to H-zeaxanthin, the 30 ps component is assigned to the S_1 lifetime of J-zeaxanthin. Although interaction between neighboring molecules in J-zeaxanthin is weaker than for H-zeaxanthin, J-zeaxanthin contains larger aggregates than H-zeaxanthin, which may lead to further decrease of the vibrational coupling via the C═C vibrational mode, explaining the even longer S_1 lifetime of J-zeaxanthin. On the other hand, it is necessary to keep in mind that for both J- and H-zeaxanthin there is a certain distribution of aggregate sizes and consequently a distribution of S_1 lifetimes, because the vibrational coupling will be more affected for large aggregates. Therefore, the observed S_1 lifetimes represent mean values and the difference between J- and H- aggregates may simply reflect the fact that the center of the distribution is shifted toward smaller aggregates for H-zeaxanthin.

Besides the vibrational coupling, a change in the S_1 energy due to aggregation should be also considered as a possible origin of different S_1 lifetimes, as these two parameters are directly related.[2] However, due to the forbidden nature of the S_1 state, the changes in the S_1 energy induced by aggregation will be much smaller than for the strongly allowed S_2 state. The fact that the ESA band corresponding to the S_1-S_N transition for monomeric and H-zeaxanthin peaks at the same wavelengths (Figure 5a) supports this conclusions. Since the higher excited states are also only a little affected by H-type aggregation (see Figure 4), the identical position of the S_1-S_N transitions of zeaxanthin and H-zeaxanthin implies negligible change in the S_1 energy upon aggregation. On the contrary, the J-type aggregation shifts the higher excited states to lower energy (Figure 4). Thus if the S_1 energy remains the same, the S_1-S_N transition should be red-shifted, exactly as observed in our experiments. Therefore, we conclude that the S_1 energy is only marginally affected by both types of aggregation and that the changes in the S_1 lifetimes are related solely to a perturbation of the vibrational coupling.

A similar argument can hardly be applied to explain the presence of the long decay component (>500 ps) for H-zeaxanthin. Even for large H-zeaxanthin assemblies, solely the vibrational coupling cannot account for such a dramatic change of the S_1 lifetime. Moreover, if a fraction of the H-zeaxanthin had a S_1 lifetime of >500 ps, the sample should be fluorescing, because short carotenoids with a comparable S_1 lifetime exhibit pronounced S_1 emission.[37] Since we have not detected any emission of H-zeaxanthin in the spectral region 500−790 nm (excitation at 400 nm, data not shown), the >500 ps decay component can hardly be associated with the S_1 lifetime. In addition, transient absorption spectra recorded at 150 ps (Figure 10) shows that the ESA profile is different at longer delays, which is also supported by the fitting results in Table 1 showing

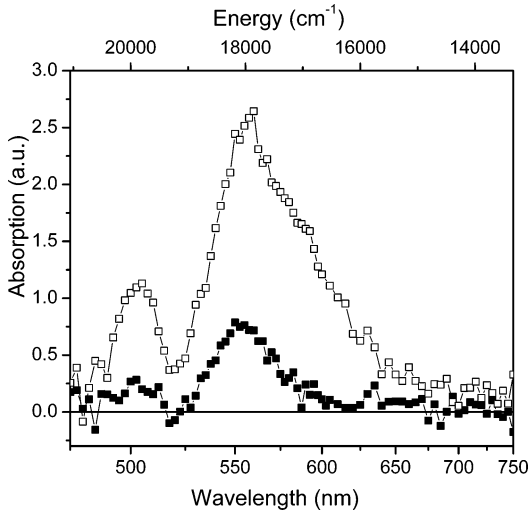

Figure 10. Transient absorption spectra of H-zeaxanthin recorded at 3 ps (□) and 150 ps (■) after excitation at 400 nm.

that the long decay component is missing in the red part of the transient absorption spectrum. On the other hand, the shape of the ESA band at 150 ps delay is, apart from a slight red shift that may be caused by aggregation, reminiscent of the spectrum of the zeaxanthin triplet.[38] The lifetime of a carotenoid triplet is usually on the microsecond time scale, justifying the presence of the long decay component. Thus, we propose that the long decay component is likely due to the formation of the zeaxanthin triplet state in H-aggregates. Observation of the triplet state only for H-zeaxanthin may be related to the specific interaction among molecules within the H-type aggregate, because enhancement of intersystem crossing upon aggregation of certain dyes has been suggested nearly 50 years ago.[39] Interestingly, however, the annihilation data suggest that the triplet state cannot be formed from the S_1 state, because the amplitude of the >500 ps component is independent of excitation intensity, and therefore insensitive to annihilation. Thus, the triplet state should be formed from another excited state. Such a scenario has been already observed, as the S* state was shown to be a precursor of ultrafast carotenoid triplet-state formation in light-harvesting complexes,[40,41] and also the $1B_u^-$ state was proposed to be a potential precursor.[42] Both these states are, for zeaxanthin in solution, likely located between the S_1 and S_2 states.[2]

Relation to Possible Functions. An important question is how these results are related to possible functions of carotenoid aggregates in natural and artificial systems. The striking similarity of J-zeaxanthin absorption spectra measured here and those obtained after incubation of zeaxanthin with either PsbS[11] or GSTP1[12] proteins allows the conclusion that in both cases the zeaxanthin−protein interaction induces formation of a head-to-tail assembly. Besides the red band characteristic of J-zeaxanthin, the red shift of the high-energy absorption band of zeaxanthin from 278 to 298 nm upon J-aggregation is also well reproduced in both zeaxanthin−protein complexes.[11,12] Since binding to a protein does not allow formation of large-scale assemblies, the most likely explanation of the absorption spectra of zeaxanthin−PsbS and zeaxanthin−GSTP1 complexes is a protein-induced formation of a head-to-tail zeaxanthin dimer. This proposal is in agreement with that of Aspinall-O'Dea et al.,[11] who suggested formation of a zeaxanthin dimer in the zeaxanthin−PsbS complex. Further verification of this proposal awaits the application of time-resolved absorption spectroscopy to study the excited-state dynamics of the zeaxanthin−PsbS (or zeaxanthin−GSTP1) complex.

A time-resolved study of excited states of the zeaxanthin−PsbS and/or zeaxanthin−GSTP1 complex is also desirable for comparison of excited-state dynamics of J-zeaxanthin in different environments. The observed changes in the excited-state properties of J-zeaxanthin do not suggest that the zeaxanthin-PsbS complex should have an increased capability of direct quenching of chlorophyll excited states. If the excited-state dynamics of the zeaxanthin−PsbS protein in fact turn to be similar to that of J-zeaxanthin in hydrated ethanol, it would rather point to an indirect function of PsbS in NPQ, for example, as a zeaxanthin transport protein. Such a protein should play a role in the NPQ machinery, because a recent proposal based on the 2.4 Å structure of the LHCII complex[43] locates the quenching site at the periphery of the LHCII complex. Consequently, a transport protein is necessary to deliver zeaxanthin from the site of creation (violaxanthin deepoxidase) to the quenching site.

The results presented here also raise an interesting question concerning binding of zeaxanthin to either the PsbS or GSTP1 protein. In both proteins, the binding of zeaxanthin was induced upon incubation of zeaxanthin with protein in a buffer of slightly alkaline pH (8.0 and 7.8, respectively). Therefore, it is an interesting question whether the head-to-tail assembly was induced solely by a specific binding to the protein or if the alkaline pH somehow promotes formation of the head-to-tail assembly as observed here for J-zeaxanthin in hydrated ethanol. Nevertheless, the protein binding is apparently a key factor as shown, for example, by the interaction of zeaxanthin with the two macular proteins XBP and GSTP1, which results in absorption spectra of monomeric and J-zeaxanthin, respectively.[12] Similarly, a much weaker 535-nm band attributable to J-zeaxanthin has been found in plant mutants lacking the PsbS protein.[44] However, if a pH-dependent control of aggregation is also involved, it may have an important implication for physiological functions.

Acknowledgment. We thank Hans-Erik Åkerlund for providing us purified zeaxanthin and Jingxi Pan for technical assistance. The work at Lund University was supported by grants from the Swedish Research Council, the Wallenberg Foundation, and the Crafoord Foundation. T.P. thanks the Swedish Energy Agency for financial support.

References and Notes

(1) Britton, G. *FASEB J.* **1995**, *9*, 1551.
(2) Polívka, T.; Sundström, V. *Chem. Rev.* **2004**, *104*, 2021.
(3) Holt, N. E.; Fleming, G. R.; Niyogi, K. K. *Biochemistry* **2004**, *43*, 8281.
(4) Edge, R.; McGarvey, D. J.; Truscott, T. G. *J. Photochem. Photobiol. B* **1997**, *41*, 189.
(5) Pincemail, J. In *Analysis of Free Radicals in Biological Systems*; Favier, A. E., Cadet, J., Kalyanaraman, B., Fontecave, M., Pierre, J.-L., Eds.; Birkhauser Verlag: Basel, Switzerland, 1995.
(6) Ruban, A. V.; Horton, P.; Young, A. J. *J. Photochem. Photobiol. B* **1993**, *21*, 229.
(7) Simonyi, M.; Bikadi, Z.; Zsila, F.; Deli, J. *Chirality* **2003**, *15*, 680.
(8) Gruszecki, W. I. In *Photochemistry of Carotenoids*; Frank, H. A., Young, A. J., Britton, G., Cogdell, R. J., Eds.; Kluwer Academic Publishers: Dordrecht, The Netherlands, 1999; p 363.
(9) Zsila, F.; Bikádi, Z.; Keresztes, Z.; Deli, J.; Simonyi, M. *J. Phys. Chem. B* **2001**, *105*, 9413.
(10) Schindler, C.; Lichtenthaler, H. K. *J. Plant. Physiol.* **1996**, *148*, 399.
(11) Aspinall-O'Dea, M.; Wentworth, M.; Pascal, A.; Robert, B.; Ruban, A.; Horton, P. *Proc. Natl. Acad. Sci. U.S.A.* **2002**, *99*, 16331.
(12) Bhosale, P.; Larson, A. J.; Southwick, K.; Thulin, C. D.; Bernstein, P. S. *J. Biol. Chem.* **2004**, *279*, 49447.
(13) Baró, A. M.; Hla, S.-W.; Rieder, K. H. *Chem. Phys. Lett.* **2003**, *369*, 240.
(14) Pan, J.; Xu, Y.; Sun, L.; Sundström, V.; Polívka, T. *J. Am. Chem. Soc.* **2004**, *126*, 3066.
(15) Sereno, L.; Silber J. J.; Otero, L.; del Valle Bohorquez, M.; Moore, A. L.; Moore, T. A.; Gust, D. *J. Phys. Chem.* **1996**, *100*, 814.
(16) Gao, F. G.; Bard, A. J.; Kispert, L. D. *J. Photochem. Photobiol. A* **2000**, *130*, 49.
(17) Pan, J.; Benkö, G.; Xu, Y.; Pascher, T.; Sun, L.; Sundström, V.; Polívka, T. *J. Am. Chem. Soc.* **2002**, *124*, 13949.
(18) Ramachandran, G. K.; Tomfohr, J. K.; Li, J.; Sankey, O. F.; Zarate, X.; Primak, A.; Terazono, Y.; Moore, T. A.; Moore, A. L.; Gust, D.; Nagahara, L. A.; Lindsay, S. M. *J. Phys. Chem. B* **2003**, *107*, 6162.
(19) Ruban, A. V.; Pascal, A. A.; Robert, B.; Horton, P. *J. Biol. Chem.* **2002**, *277*, 7785.
(20) Li, X.-P.; Björkman, O.; Shih, C.; Grossman, A. R.; Rosenquist, M.; Jansson, S.; Niyogi, K. K. *Nature* **2000**, *403*, 391.
(21) Ma, Y.-Z.; Holt, N. E.; Li, X.-P.; Niyogi, K. K.; Fleming, G. R. *Proc. Natl. Acad. Sci. U.S.A.* **2003**, *100*, 4377.
(22) Yemelyanov, A. Y.; Katz, N. B.; Bernstein, P. S. *Exp. Eye. Res.* **2001**, *72*, 381.
(23) Billsten, H. H.; Bhosale, P.; Yemelyanov, A.; Bernstein, P. S.; Polívka, T. *Photochem. Photobiol.* **2003**, *78*, 138.
(24) Sujak, A.; Mazurek, P.; Gruszecki, W. I. *J. Photochem. Photobiol. B* **2002**, *68*, 39.
(25) Cantrell, A.; McGarvey, D. J.; Truscott, T. G.; Rancan, F.; Böhm, F. *Arch. Biochem. Biophys.* **2003**, *412*, 47.
(26) Polívka, T.; Zigmantas, D.; Sundström, V.; Formaggio, E.; Cinque, G.; Bassi, R. *Biochemistry* **2001**, *41*, 439.
(27) Frank, H. A.; Cua, A.; Chynwat, V.; Young, A.; Gosztola, D.; Wasielewski, M. R. *Photos. Res.* **1994**, *41*, 389.
(28) Billsten, H. H.; Zigmantas, D.; Sundström, V.; Polívka, T. *Chem. Phys. Lett.* **2002**, *355*, 465.
(29) Gruszecki, W. I. *J. Biol. Phys.* **1991**, *18*, 99.
(30) Martin, H. D.; Werner, T. *J. Mol. Struct.* **1992**, *266*, 91.
(31) Wang, Y.; Mao, L.; Hu, X. *Biophys. J.* **2004**, *86*, 3097.
(32) Sundström, V.; Gillbro, T. *J. Chem. Phys.* **1985**, *83*, 2733.
(33) Khairutdinov, R. F.; Serpone, N. *J. Chem. Phys. B* **1997**, *101*, 2602.
(34) Sundström, V.; Gillbro, T.; Gadonas, R. A.; Piskarskas, A. *J. Chem. Phys.* **1988**, *89*, 2754.
(35) Trinkunas, G.; Herek, J. L.; Polívka, T.; Sundström, V.; Pullerits, T. *Phys. Rev. Lett.* **2001**, *86*, 4167.
(36) Nagae, H.; Kuki, M.; Zhang, J.-P.; Sashima, T.; Mukai, Y.; Koyama, Y. *J. Phys. Chem. A* **2000**, *104*, 4155.
(37) Christensen, R. L.; Goyette, M.; Gallagher, L.; Duncan, J.; DeCoster, B.; Lugtenburg, J.; Jansen, F. J.; van der Hoef, I. *J. Phys. Chem. A* **1999**, *103*, 2399.
(38) Nielsen, B. R.; Mortensen, A.; Jørgensen, K.; Skibsted, L. H. *J. Agric. Food Chem.* **1996**, *44*, 2106.
(39) McRae, E. G.; Kasha, M. *J. Chem. Phys.* **1958**, *28*, 721.
(40) Gradinaru, C. C.; Kennis, J. T. M.; Papagiannakis, E.; van Stokkum, I. H. M.; Cogdell, R. J.; Fleming, G. R.; Niederman, R. A.; van Grondelle, R. *Proc. Natl. Acad. Sci. U.S.A.* **2001**, *98*, 2364.
(41) Papagiannakis, E.; Kennis, J. T. M.; van Stokkum, I. H. M.; Cogdell, R. J.; van Grondelle, R. *Proc. Natl. Acad. Sci. U.S.A.* **2002**, *99*, 6017.
(42) Rondonuwu, F. S.; Watanabe, Y.; Fujii, R.; Koyama, Y. *Chem. Phys. Lett.* **2003**, *376*, 292.
(43) Liu, Z. F.; Yan, H. C.; Wang, K. B.; Kuang, T. Y.; Zhang, J. P.; Gui, L. L.; An, X. M.; Chang, W. R. *Nature* **2004**, *428*, 287.
(44) Horton, P.; Ruban, A. V.; Wentworth, M. *Philos. Trans. R. Soc. London B* **2000**, *355*, 1361.